TECHNICAL PAPERS

NUMERICAL INVESTIGATION OF DEBONDING ON PIEZO-ELASTIC SYSTEM USING COUPLED FIELD ANALYSIS

Deepak V V N S S[1] and Sumedha Moharana[1]

[1] Graduate Student, Department of Civil Engineering, Shiv Nadar University, Dadri-201314, Email-dv638@snu.edu.in

[2]Associate Professor, Department of civil engineering, Shiv Nadar University, Dadri-201314, Email-sumedha_maharana@snu.edu.in

Abstract. For the past few years, along with the increasing population growth the demand for the Civil Engineering structures has increased drastically. For safety and serviceability requirement the performance of these structures must be monitored periodically. Structural Health Monitoring (SHM) provides best periodic checks for measuring or sensing the response by using different types of smart materials which responds to different parameters like stress, magnetic field, electric field, heat etc. In general, EMI signature depends on the adhesive that is used to glue the PZT patch and the host structure. Any change in adhesive material might also be a cause for the deflections in the overall signature as the stress transfer occurs through the bonding layer. This paper aims to investigate the de-bonding effect of adhesive layer on the efficiency of damage detection of PZT when bonded to structure to be monitored. The Finite element (FE) coupled analysis for smart structural system i.e for aluminium beam attached to PZT patch with adhesive bond with different de-bonding geometry. The numerical results are compared with the results of perfect bonding condition to highlight the efficiency of developed model.

Keywords: Piezoelectric patch, Sensor, bond, adhesive, Electro-mechanical impedance technique, Coupled Field Analysis

1. Introduction

Electro Mechanical Impedance (EMI) is considered to be one of the best cost effective techniques in SHM, which exhibit high damage sensitivity and high performance. During the recent past, piezoelectric patches are the most common devices that are used as high frequency mechatronics transducers for Structural health Monitoring (SHM).

The PZT transducers are easily surface-bonded to the host structure to obtain the baseline coupled admittance signature of the structure which is function of structural impedance. Due to self-sensing mechanism, when they are subjected to high frequency excitations of electric field by using impedance analyser or LCR meter and the admittance signatures obtained consists of conductance as real part and susceptance as imaginary part. This obtained baseline signature is used to compare and analyse about the existing condition of the structure and further anomalies. Any damage in the host structure will cause significant change in mechanical impedance of the structure which in turn modifies the actual admittance signatures obtained from the PZT transducer. As the PZT patch is directly bonded to the structure, the mechanical impedance of the structure correlates with the electrical impedance of the patch [1]

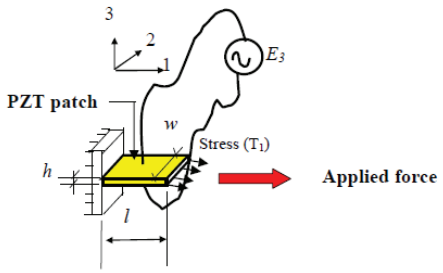

Figure. 1. EMI Technique of PZT patch

A Coupled-field analysis (CFA) is a type of analysis in which two or more than two different engineering disciplines (Fields) are combined together to solve a global problem and so it is referred as Multi-physics analyses. In much simpler terms, it can be said that the result of one field directly depends on the input of the other field or

vice-versa. These analyses can be of either one-way or two-way analyses. Two way is more complicated compared to the one way as the iteration has to be done for different fields involved in the analysis.

In general, CFA is of two types based on which fields are bring coupled: (a) Load Transfer Method and (b) Direct Method. Load transfer method is used when two or more analyses has to be done in which each analysis belongs to different fields are involved [**2,3**]. So coupling is done between two fields by applying the results of one field in the analysis as loads in the other analysis. Piezoelectric analysis belongs to direct method coupled-field analysis in which only one analysis is done using a coupled-field element type which consists of all necessary degrees of freedom. In

Numerical modelling of PZT-5H soft ceramic model piece using CFA in Finite element software ANSYS shows the voltage obtained from positive piezoelectric effect (sensor function) and displacement from secondary converse piezo electric effect (actuator function) [**4**]. A detailed comparison of damage assessment between different types of PZT patch configuration such as (a) SPC (Single Piezo Configuration), which is conventionally used in EMI technique, (b) DPC (Dual Piezo Configuration, which consists of ring type of patches, (c) MDPC (Modified Dual Piezo Configuration) which uses 4 outer piezo patches as actuators and a centrally placed piezo patch as a sensor shows the improved sensitivity and accurate results in case of MDPC (Adhikari and Bhalla, 2019) **[5]**.

A bonding layer is used to embed a PZT on to the host structure, which plays a crucial role in transferring stresses and strains from PZT patch to host structure and vice-versa. Therefore, the existence of bond layer introduces the shear lag effect, as a result of which the strain induced in the PZT patch is different from that on the surface of the host structure. Shear lag effect is the phenomenon caused due to piezo deformation (actuation/sensing) transferred to the structure via adhesive bond. Practically, it is impossible to introduce uniform bonding layer (constant thickness and required dimensions) into the system and also reduction in dimensions of bonding layer might enhance the output signatures as they provide resistance to the stress transfer.

This paper includes the numerical modelling of sensor-structural system (aluminium beam with bonded PZT patch) using coupled field analysis. Different de-bonding geometries of bonding layer are introduced between the PZT patch and the host structure and obtained the coupled admittance signatures which are compared against the actual conventional epoxy adhesive bond layer system's admittance signatures to analyse the sensitivity of developed model and it's accuracy to warrant the debonding in overall sensor response.

2. Numerical Modelling

The modelling of the system was done using ANSYS software version [6]. SOLID 45 and SOLID 5 were considered as the element types for the structure and the PZT patch respectively. 1/2nd of an Aluminium block/beam of dimensions of 200mm×20mm×6mm with conventional PZT patch of dimensions 10mm×10mm×0.3mm was considered for modelling in order to minimize the computation time with the benefit geometrical symmetry. The material properties of the Aluminium block are listed in table 1 and those of PZT are mentioned in table 2.

Table 1. Properties of Specimen (aluminium block)

Modulus of elasticity (E)	68.95 GPa
Poisson ratio (ν)	0.33
Density (ρ)	2715 kg/m^3
Mass damping factor (α)	0
Stiffness damping factor (β)	3×10^{-9}

Table 2. Properties of Piezoelectric Patch (PZT)

Parameters	Symbols	Values	Unit
Density	ρ	7800	Kg/m^3
Dielectric loss factor	Tanδ	0.02	
Compliance	S_{11}	15.0	

	$S_{22}=S_{23}$	19.0	10^{-12} m^2/N
	$S_{12}=S_{21}$	-4.50	
	$S_{13}=S_{31}$	-5.70	
	$S_{23}=S_{32}$	-5.70	
	$S_{44}=S_{55}$	39.0	
	S_{66}	49.4	
Electric Permittivity	ε_{11}^{T}	1.75	10^{-8}F/m
	ε_{22}^{T}	1.75	
	ε_{33}^{T}	2.12	
Piezoelectric Strain Coefficients	d_{31}	-2.10	10^{-10} m/V
	d_{32}	-2.10	
	d_{33}	5.0	
	d_{24}	5.80	
	d_{15}	5.80	

The de-bonding configuration for the adhesive bonding layer is modelled for each de-bonding case i.e. w.r.t to percentage (%) of bonding layer area is reduced based on the geometry chosen. Figure 2 represents different de-bonding geometries that are used in this research. “Glue” command was used to combine two materials as one entity and to ensure that there exists full connection between PZT and host structure (Aluminium beam). The system is uniformly meshed with 1mm as global meshing size [7]. The sensor-structural system (PZT patch & Aluminium) is applied with boundary conditions such as structural displacements (Degrees of Freedom) on the required areas and the electric boundary conditions on top and bottom surfaces of the PZT patch were applied with a voltage difference of 1 volt i.e. Top surface with 1 volts and bottom surface with 0 volts. Both Top and bottom surfaces of the PZT patch were coupled by ‘VOLT’ DOF. During coupling, one of the node is mastered on the top surface and one of the node is mastered on the bottom surface of the PZT patch. The output data was obtained by acquiring current values from mastered node only.

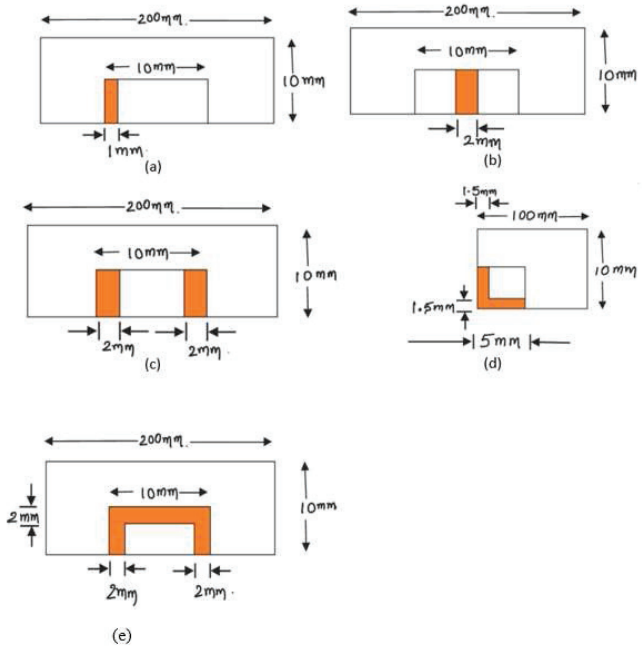

Figure. 2. De-bonding Geometry of adhesive bond layer with (a) 10% reduction in bond area; (b) 20% reduction in bond area; (c) 40% reduction in bond area; (d) 51% reduction in bond area; (e) 64% reduction in bond area.

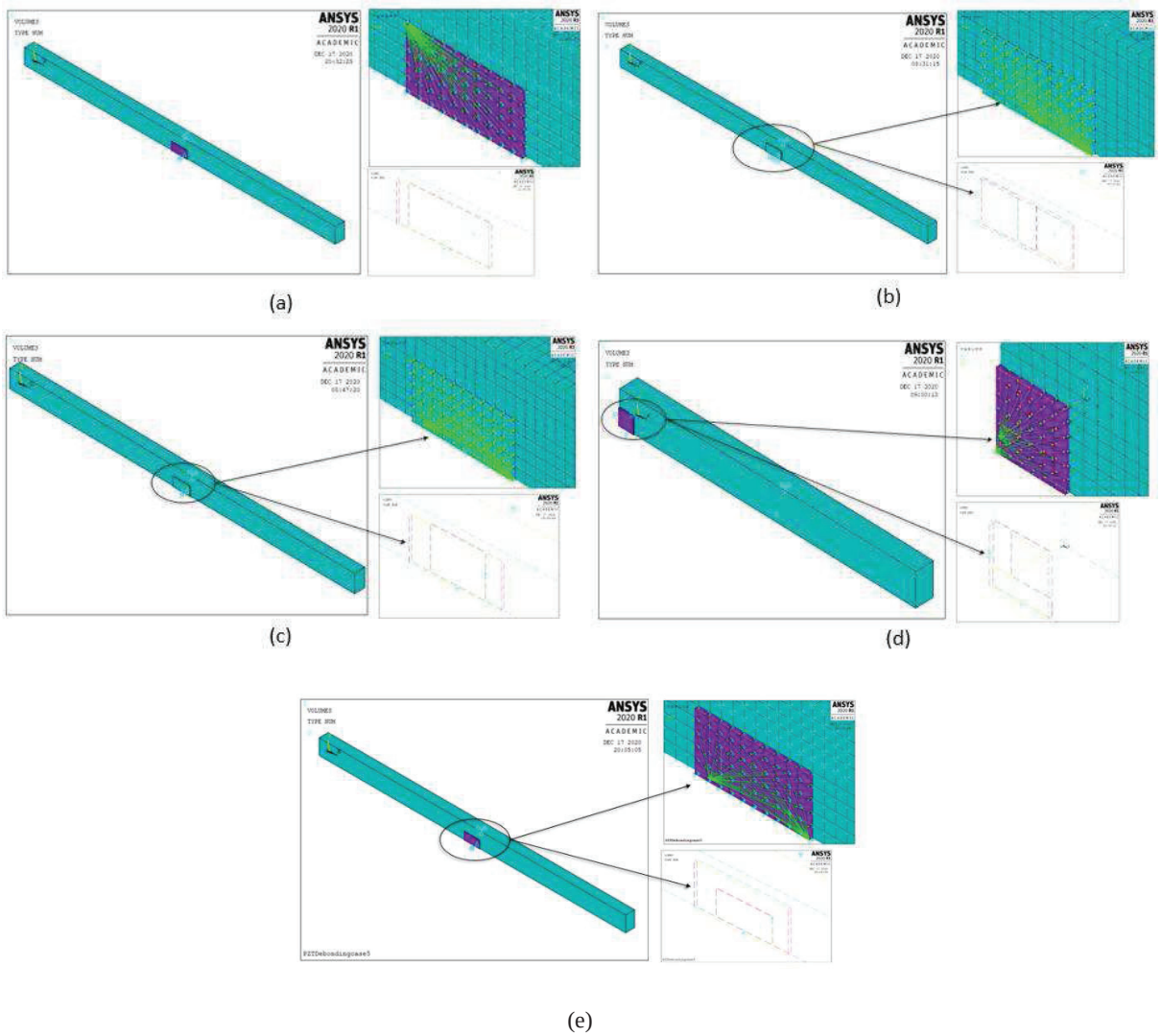

Figure. 3. FE modelling of SPC and Aluminium beam with adhesive bonding layer of (a) 10% de-bonding area; (b) 20% de-bonding area; (c) 40% de-bonding area; (d) 51% de-bonding area; (e) 64% de-bonding area.

Figure 3 represents the numerical modelling of different de-bonding geometries with different bond areas in ANSYS 2020 R1. Dynamic harmonic analysis for frequency range of 0-1000 kHz with an interval of 1 kHz frequency was performed to obtain the charge as output. Stiffness damping factor (β) = 3×10^{-9} is provided to the PZT patch. Current flow labelled as AMPS was measured as reaction forces along top mastered node of the PZT patch from the time history postprocessor of ANSYS. The output data obtained was negative of the charge (-Q) and the value of current flow obtained can be expressed as:

$$I = \frac{d(-Q)}{dt} = -j\omega Q \tag{1}$$

Current flow consists of real and imaginary parts *[-(a+bj)]*. Since the output obtained from time history post processor is negative of current flow, the value of current *'I'* can be written as

$$I = -j\omega(a + bj) \tag{2}$$

$$I = (-aj + b)\omega \tag{3}$$

It can be observed from equation (3) that the real part of current flow will contribute to the imaginary component and the imaginary part of current flow will contribute to the real component of the current. The difference between the current from the top and the bottom node is considered and so the output current *(I_{out})* which consists of real and imaginary components is obtained.

3. Results and Discussion

It is observed that magnitude of highest peak value for conductance signatures of different types of de-bonding geometries is shown in figure 4(a). From figure 4(b), the difference in slope value of all the susceptance signatures varies because the reactive component of signature dominated with adhesive bond properties. Since the active component depends on the properties of both PZT and structure and also the mechanical impedance of the structure couples with the mechanical impedance of the PZT patch only in the active component, the magnitude of the peak and the change in slope of the signatures occurs due to bond properties.

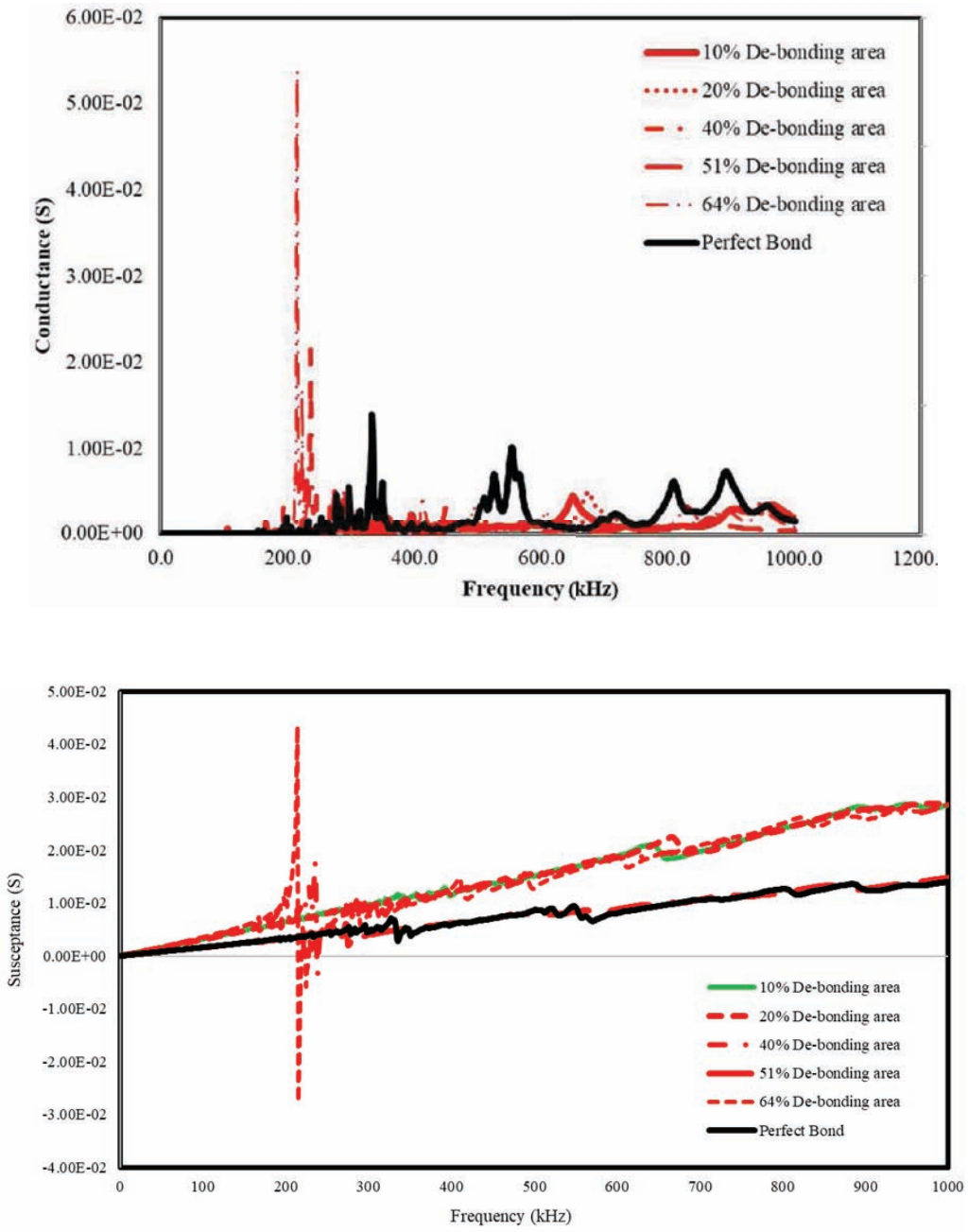

Figure 4. Comparison of admittance signatures for SPC and Aluminium block with adhesive bonding layer of different de-bonding geometries with Perfect bonding condition

(a) Conductance Vs Frequency
(b) Susceptance Vs Frequency

In overall, it can be concluded that with increasing of bond degraded area, the frequency of conductance signature increases but not in steady manner (see Fig 4a). However, the conductance peak value increases significantly,

quite similar to PZT signature in free-free condition. In susceptance, the effect is more evitable with change in slope of the signature curve and peak values (see Fig 4b).

In EMI technique, RMSD index is the most commonly used to detect the quantitative structural damage by computing the degree of deviation of the admittance signatures from the de-bonded PZT-structural system to the base line (complete bond area) signatures. The RMSD index can be expressed mathematically as [8] :

$$RMSD(\%) = \sqrt{\frac{\sum_{j=1}^{N}(G_j^1 - G_j^0)^2}{\sum_{j=1}^{N}(G_j^0)^2}} \times 100 \qquad (4)$$

where G_j^1 is the conductance of de-bonded geometry at j[th] frequency and G_j^0 is the conductance of pristine state at same j[th] frequency.

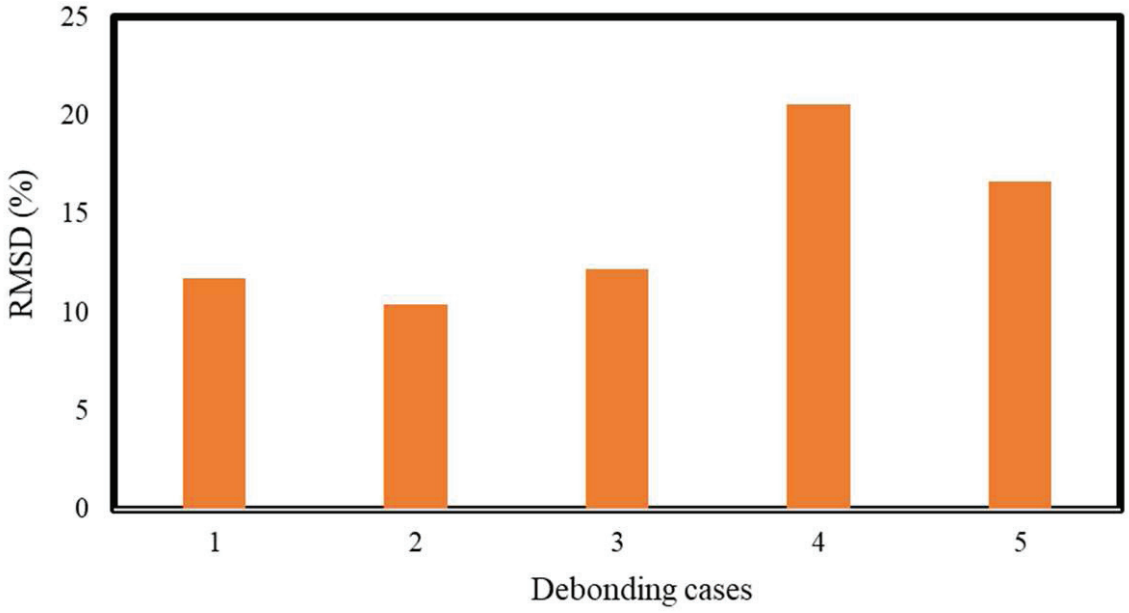

Figure. 5. Variation of RMSD for different case of debonded configuration for sensor-structural system

From figure 5, it is observed that RMSD % varies in significant amount in case of conductance signatures which states that the shift in magnitude of peaks from its pristine state is considerable i.e. the peak values occur at different frequency values and it varies in each case. De-bonding case 4 (51% reduction in bond area) shows the highest RMSD value. It implies the decoupling of sensor-structure is initiated at that stage.

4. Conclusion

It can be concluded from the observations made for all five de-bonding geometry cases that the overall the peak magnitude increases as area of de-bonding decreases and in general, the peaks shift towards right as area of de-bond increases. But for case 5 (64% reduction in area of bonding layer), maximum peak value occurs at around 210 kHz which is similar to that of PZT's for free-free condition (occurs at around 180 kHz) but with reduction in magnitude of the peak. No. of peaks in numerical signatures are less and it might be due to: (i) The damping introduced in the numerical simulation; and (ii) there will be no chemical reactions in bond during Numerical simulation as that in case of experimental setup due to surrounding environmental exposure. The de-bonding effect of adhesive layer on the efficiency of damage detection of PZT when bonded to structure is monitored. The Finite element (FE) coupled analysis is done for aluminium block attached to PZT patch with different de-bonding geometries. Damage sensitivity is analysed and the numerical results are compared with the perfect bonding condition.

5. References

1. Liang, C., Sun, F. P., Rogers, C. A. Coupled Electro-Mechanical Analysis of Adaptive Material Systems-Determination of the Actuator Power Consumption and System Energy Transfer. Journal of Intelligent Material Systems and Structures, 8, 335-343 (1997).
2. Gopalakrishnan, S., Ruzzene, M.,Hanaguad, S. Spectral Finite Element Method. Springer-Germany, (2008).
3. Gopalakrishnan, S., Ruzzene, M.,Hanaguad, S. Computational Techniques for Structural Health Monitoring. Springer –UK, (2011).
4. Lijing, W., Liping, S. Simulation of the self-sensing actuators based on multi-piezoelectric effects of piezoelectric crystal. Proceedings of 2011 International Conference on Electronic & Mechanical Engineering and Information Technology, IEEE, 1876-1879 (2011).
5. Adhikari, S., Bhalla, S. Modified Dual Piezo Configuration for Improved Structural Health Monitoring Using Electro-Mechanical Impedance (EMI) Technique. Experimental Techniques, 43, 25-40 (2019).
6. ANSYS ANSYS VERSION 2020R1, http://www.ansys.com (2020) .
7. Moharana, S. Modelling of piezo-structure elastodynamic interaction through bond layer for electro-mechanical impedance technique (2012).
8. Bhalla, S. A mechanical impedance approach for structural identification, health monitoring and non-destructive evaluation using piezo-impedance transducers. Nanyang Technological University, School of Civil & Environmental Engineering (2004).